A Novel Multi Regional Reliability Method for COVID-19 Death Forecast

Oleg Gaidai[1], Yihan Xing[2,*]

[1] *Shanghai Ocean University, Shanghai, China*
[2] *University of Stavanger, Norway*

*** *E-mail**: yihan.xing@uis.no*

Abstract

Novel coronavirus disease is spread worldwide with considerable morbidity and mortality and presents an enormous burden on worldwide public health. The present study describes a novel bio-system reliability approach, particularly suitable for multi-regional environmental and health systems, observed over a sufficient period, resulting in a reliable long-term forecast of the novel coronavirus death rate. To determine extreme novel coronavirus death rate probability at any time in any region of interest. Traditional statistical methods dealing with temporal observations of multi-regional processes do not have the advantage of dealing efficiently with extensive regional dimensionality and cross-correlation between different regional observations. The present study presents a novel statistical method to analyse raw clinical data using a multicenter, population-based, medical survey data-based biostatistical approach. Due to the non-stationarity and complicated nature of the novel coronavirus, it is challenging to model such a phenomenon. The present study describes a novel bio-system reliability approach, particularly suitable for multi-region environmental and health systems, observed over a sufficient period, resulting in a reliable long-term forecast of extreme novel coronavirus death rate probability. The method also indicates the accuracy by presenting the 95% confidence interval band. The suggested methodology can be used in various public health applications based on their clinical survey data.

Keywords: COVID-19; Epidemic outbreak; Probability forecast; Public health; Mathematical biology.

1. Review

Statistical aspects of COVID-19 and other similar recent epidemics were receiving much attention in the modern research community[1]-[4]. Generally, it is relatively challenging to calculate realistic biological system reliability factors and outbreak probabilities under actual epidemic conditions using conventional theoretical statistical methods[4]-[20]. The latter is usually due to many degrees of system freedom and random variables governing dynamic biological and health systems[22],[23]. In principle, the reliability of a complex biological system may be accurately estimated straightforwardly by having enough measurements or by direct Monte Carlo simulations. For COVID-19, however, the only available observation numbers are limited by the beginning of the year 2020. Motivated by the latter argument, the authors have introduced a novel reliability method for biological and health systems to predict and manage epidemic outbreaks more accurately. This study focused on COVID-19 epidemics in Israel, focusing on cross-correlations between different health records within the same climatic zone. Israel was chosen, of course, because of its COVID-19 origin and extensive health observations and related research available online [24]-[37]. For other studies related to statistical variations per country, see[24].

Statistical modelling of lifetime data or extreme value theory (EVT) is widespread in medicine or engineering. For example, Gumbel used EVT to estimate the demographic of various populations. Often, papers in these fields presume a parametric bivariate lifetime distribution obtained from the exponential distribution to get statistically relevant data[38]. In [19], the author proposes a new approach that uses Power Variance Function copulas (e.g., Clayton, Gumbel and Inverse Gaussian copulas), conditional sampling, and numerical approximation used in survival analysis. Finally, [19] is a paper of relevance which used EVT to estimate the probability of an influenza outbreak in Israel. The authors demonstrated a forecasting prediction potential amid the epidemic. While [20] similarly used EVT to predict and detect anomalies of influenza epidemics. As there is not much statistical research done to predict the probability of influenza or contagious diseases outbreak or their spread, the proposed new method will provide better insight and an indication of the possible spread of diseases.

Using two simple mathematical epidemiological models, the Susceptible-Infectious-Recovered model and the log-linear regression model, the authors in [39] modelled daily and cumulative incidence of COVID-19 in the two countries during the early stage of the outbreak. Other studies include analysis of the spatial variability of the incidence using spatial lag and error models and geographically weighted regression[40].

2. Introduction

In the present study, an epidemic outbreak was viewed as an unexpected incident that may occur in any country's health system category at any time. Therefore, the spatial spread is accounted for. Moreover, a specific non-dimensional factor λ is introduced to predict the latter epidemic risk at any time and place.

Biological systems are subjected to ergodic environmental influences. The other alternative is to view the process as dependent on specific environmental parameters whose variation in time may be modelled as an ergodic process on its own.

The incidence data of COVID-19 in Israel from February 2020 until today were retrieved from the public website[1]. As this valuable data set is from Israel, the biological system under consideration can be regarded as a multi-degree of freedom (MDOF) dynamic system with highly inter-correlated observational components/dimensions. Some recent studies have already used statistical tools to predict COVID-19 development for the linear log model see[39].

Note that while this study aims to reduce the risk of future epidemic outbreaks by predicting them, it focuses solely on daily registered patient numbers and not symptoms. For long-lasting COVID-19 symptoms, the so-called "long COVID" and its risk factors and whether it is possible to predict a protracted course early in the disease. Fig. 1 presents a map of Israel; black dots represent individual cases.

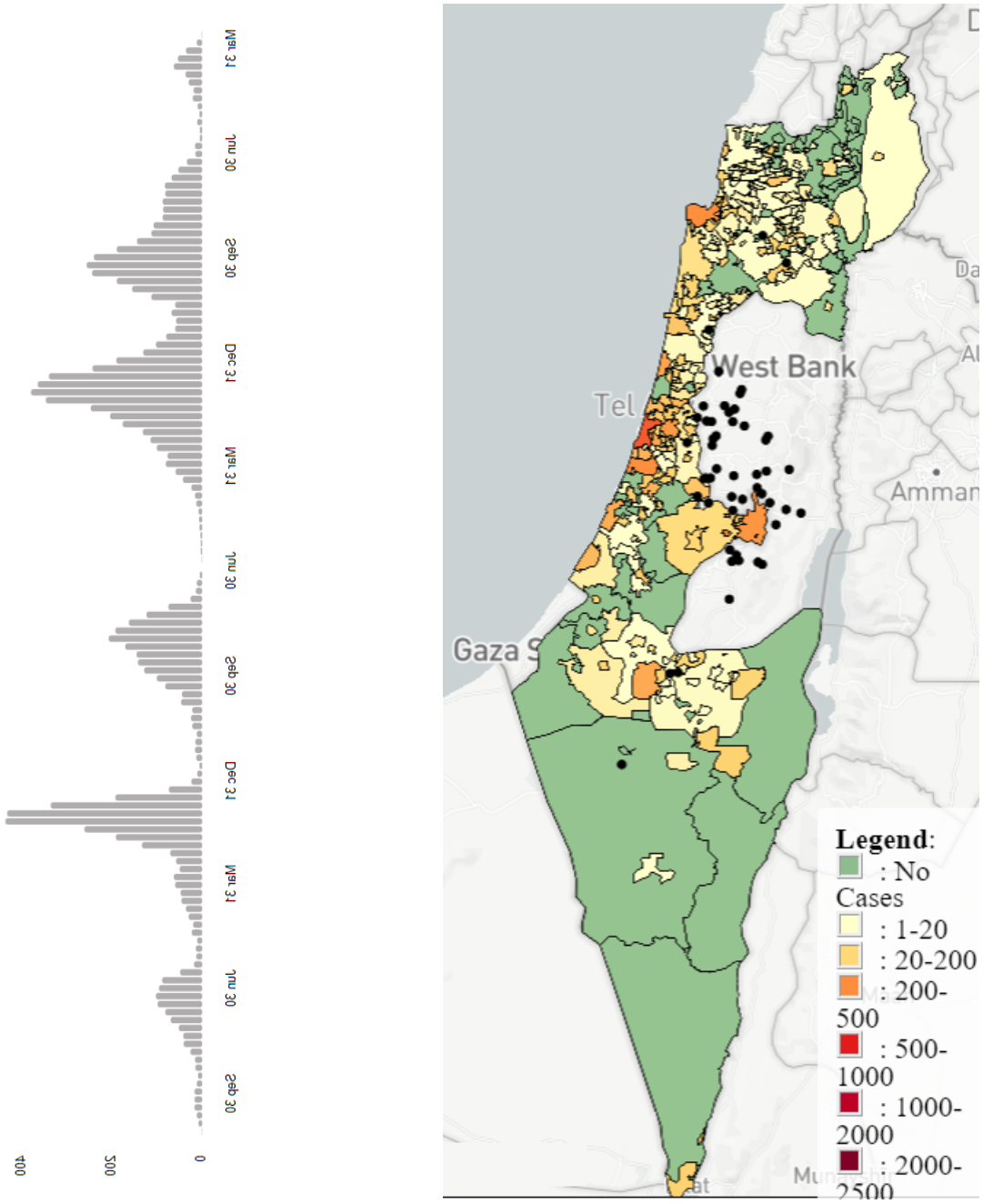

Fig. 1 Left: COVID death cases in Israel[2]; Right: map of Israel with registered COVID cases[3].

This study relied on the quasi-stationarity assumption; the underlying epidemiological process was assumed, although seasonally varying but still statistically representative during two 2020-2022 years of continuous observation. The underlying trend must be addressed in the longer time horizon, for example, 10-100 years. Note that although analysed data set is quite limited both in time (only two years) as well as in space (only state of Israel), the proposed methodology has already been well validated in other studies by authors[8].

3. Methods and materials

The MDOF health response vector process $\boldsymbol{R}(t) = (X(t),\ Y(t),\ Z(t),\ \dots)$ that has been measured over a sufficiently long time interval $(0, T)$. Unidimensional global maxima over the entire period $(0, T)$ denoted as $X_T^{\max} = \max_{0\le t\le T} X(t)$, $Y_T^{\max} = \max_{0\le t\le T} Y(t)$, $Z_T^{\max} = \max_{0\le t\le T} Z(t)$, ... see Fig. 2. By sufficiently long time T one primarily means a large value of T with respect to the dynamic system auto-correlation time. Let $X_1, \dots, X_{N_X}$ be consequent in time local maxima of the process $X(t)$ at discrete monotonously increasing time instants $t_1^X < \dots < t_{N_X}^X$ in $(0, T)$. The analogous definition follows for other MDOF response components $Y(t),\ Z(t), \dots$ with $Y_1, \dots, Y_{N_Y};\ Z_1, \dots, Z_{N_Z}$ and so on. For simplicity, all $\boldsymbol{R}(t)$ components, and therefore its maxima are assumed to be non-negative.

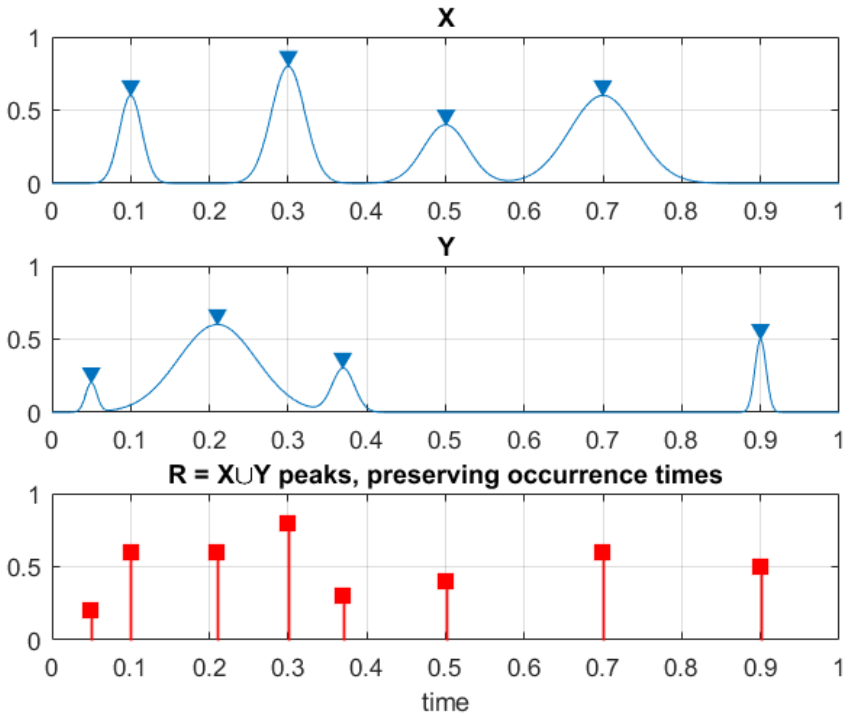

Fig. 2 Illustration of how two exemplary processes X and Y are combined into a new synthetic vector $\boldsymbol{R}(t)$. The vertical axis represents the non-dimensional λ-parameter.

The target is to estimate system failure probability, namely probability of exceedance, accurately

$$1 - P = \mathrm{Prob}(X_T^{\max} > \eta_X \ \cup\ Y_T^{\max} > \eta_Y \ \cup\ Z_T^{\max} > \eta_Z \ \cup\ \dots) \qquad (1)$$

where $P = \iiint_{(0,\ 0,\ 0,\ \dots)}^{(\eta_X,\ \eta_Y,\ \eta_Z,\ \dots)} p_{X_T^{\max},\ Y_T^{\max},\ Z_T^{\max},\dots}(X_T^{\max},\ Y_T^{\max},\ Z_T^{\max}, \dots)\, dX_T^{\max} dY_{N_Y}^{\max} dZ_{N_z}^{\max} \dots$ is the probability of non-exceedance for critical values of response components $\eta_X,\ \eta_Y,\ \eta_Z$,...; $\cup$ denotes logical unity operation «or»; and $p_{X_T^{\max},\ Y_T^{\max},\ Z_T^{\max},\dots}$ being joint probability density of the global maxima over the entire period $(0, T)$. However, it is not feasible to estimate the latter joint probability distribution directly due to its high dimensionality and available data set limitations.

More specifically, the moment when either $X(t)$ exceeds η_X, or $Y(t)$ exceeds η_Y, or $Z(t)$ exceeds η_Z, and so on, the system is regarded as immediately failed. Fixed failure levels $\eta_X,\ \eta_Y,$

η_Z,...are, of course, individual for each unidimensional response component of $\boldsymbol{R}(t)$. $X_{N_X}^{\max} = \max\{X_j; j = 1, \dots, N_X\} = X_T^{\max}$, $Y_{N_Y}^{\max} = \max\{Y_j; j = 1, \dots, N_Y\} = Y_T^{\max}$, $Z_{N_z}^{\max} = \max\{Z_j; j = 1, \dots, N_Z\} = Z_T^{\max}$, and so on.

Now, the local maxima time instants $\left[t_1^X < \cdots < t_{N_X}^X;\ t_1^Y < \cdots < t_{N_Y}^Y;\ t_1^Z < \cdots < t_{N_Z}^Z\right]$ are sorted in monotonously non-decreasing order into one single merged time vector $t_1 \le \cdots \le t_N$ .Note that $t_N = \max\{t_{N_X}^X,\ t_{N_Y}^Y,\ t_{N_Z}^Z,\ \dots\}$, $N = N_X + N_Y + N_Z + \dots$. In this case t_j represents local maxima of one of MDOF structural response components either $X(t)$ or $Y(t)$, or $Z(t)$ and so on. That means that having $\boldsymbol{R}(t)$ time record, one just needs continuously and simultaneously screen for unidimensional response component local maxima and record its exceedance of MDOF limit vector $(\eta_X,\ \eta_Y,\ \eta_Z, \dots)$ in any of its components $X, Y, Z, \dots$ Local unidimensional response component maxima are merged into one temporal non-decreasing vector $\vec{R} = (R_1, R_2, \dots, R_N)$ following the merged time vector $t_1 \le \cdots \le t_N$. That is to say, each local maxima R_j is actual encountered local maxima corresponding to either $X(t)$ or $Y(t)$, or $Z(t)$ and so on. Finally, the unified limit vector $(\eta_1, \dots, \eta_N)$ is introduced with each component η_j is either η_X, η_Y or η_Z and so on, depending on which of $X(t)$ or $Y(t)$, or $Z(t)$ etc., corresponds to the current local maxima with the running index j.

Now, scaling parameter $0 < \lambda \le 1$ is introduced to artificially simultaneously decrease limit values for all response components, namely the new MDOF limit vector $\left(\eta_X^\lambda,\ \eta_Y^\lambda,\ \eta_z^\lambda, \dots\right)$ with $\eta_X^\lambda \equiv \lambda \cdot \eta_X$, $\equiv \lambda \cdot \eta_Y$, $\eta_z^\lambda \equiv \lambda \cdot \eta_Z$, ... is introduced, see [41]. The unified limit vector $\left(\eta_1^\lambda,\ \dots,\eta_N^\lambda\right)$ is introduced with each component η_j^λ is either η_X^λ, η_Y^λ or η_z^λ and so on. The latter automatically defines probability $P(\lambda)$ as a function of λ, note that $P \equiv P(1)$ from Eq. (1). Non-exceedance probability $P(\lambda)$ can be estimated as follows

$$\begin{aligned} P(\lambda) &= \text{Prob}\{R_N \le \eta_N^\lambda, \dots, R_1 \le \eta_1^\lambda\} \\ &= \text{Prob}\left\{R_N \le \eta_N^\lambda \,\middle|\, R_{N-1} \le \eta_{N-1}^\lambda, \dots, R_1 \le \eta_1^\lambda\right\} \cdot \text{Prob}\{R_{N-1} \le \eta_{N-1}^\lambda, \dots, R_1 \le \eta_1^\lambda\} \\ &= \prod_{j=2}^{N} \text{P rob}\{R_j \le \eta_j^\lambda \mid R_{j-1} \le \eta_{1j-}^\lambda, \dots, R_1 \le \eta_1^\lambda\} \cdot \text{Prob}(R_1 \\ &\qquad \le \eta_1^\lambda) \end{aligned} \tag{2}$$

In the following, the principle behind a cascade of approximations based on conditioning is outlined. The first approximation is a one-step memory approximation and thus resembles a Markov chain approximation. However, it is emphasised that this first approximation is not equivalent to such an approximation.

In practice, the dependence between the neighbouring R_j is not negligible; thus, the following one-step (will be called conditioning level $k = 1$) memory approximation is introduced

$$\begin{aligned} \text{Prob}\{R_j \le \eta_j^\lambda \mid R_{j-1} \le \eta_{j-1}^\lambda, \dots, R_1 \le \eta_1^\lambda\} \approx \text{Prob}\{R_j \\ \le \eta_j^\lambda \mid R_{j-1} \le \eta_{j-1}^\lambda\} \end{aligned} \tag{3}$$

for $2 \le j \le N$ (conditioning level $k = 2$). The approximation introduced by Eq. (3) can be further expressed as

$$\text{Prob}\{R_j \le \eta_j^\lambda \mid R_{j-1} \le \eta_{j-1}^\lambda, \dots, R_1 \le \eta_1^\lambda\} \approx \text{Prob}\{R_j \le \eta_j^\lambda \mid R_{j-1} \le \eta_{j-1}^\lambda, R_{j-2} \le \eta_{j-2}^\lambda\} \quad (4)$$

where $3 \le j \le N$ (will be called conditioning level $k = 3$), and so on[9]-[19]. The idea is to monitor each independent failure that happened locally first in time, thus avoiding cascading local inter-correlated exceedances. Eq. (4) presents subsequent refinements of the statistical independence assumption. With increased accuracy, the latter approximations capture the statistical dependence effect between the neighbouring maxima. This study assumes the whole bio-system to be stationary, namely its dimensions to be jointly stationary, therefore the constructed process $\boldsymbol{R}(t)$ is also stationary. Since original MDOF process $\boldsymbol{R}(t)$ is ergodic and therefore stationary, probability $p_k(\lambda) \coloneqq \text{Prob}\{R_j > \eta_j^\lambda \mid R_{j-1} \le \eta_{j-1}^\lambda,\ R_{j-k+1} \le \eta_{j-k+1}^\lambda\}$ for $j \ge k$ will be independent of j but only dependent on conditioning level k. Thus non-exceedance probability can be approximated as in the average conditional exceedance rate method, see [41].

$$P_k(\lambda) \approx \exp\left(-N \cdot p_k(\lambda)\right), \qquad k \ge 1. \quad (5)$$

Note that Eq. (5) follows from Eq. (1) by neglecting $\text{Prob}(R_1 \le \eta_1^\lambda) \approx 1$, as design failure probability must be minuscule, also assumed $N \gg k$. Eq. (5) is similar to the well-known mean up-crossing rate equation for the probability of exceedance[41]. There is evident convergence with respect to the conditioning parameter k

$$P = \lim_{k\to\infty} P_k(1); \quad p(\lambda) = \lim_{k\to\infty} p_k(\lambda) \quad (6)$$

Note that Eq. (5) for $k = 1$ turns into a well-known non-exceedance probability relationship with the mean up-crossing rate function

$$P(\lambda) \approx \exp\left(-\nu^+(\lambda)\, T\right); \quad \nu^+(\lambda) = \int_0^\infty \zeta p_{R\dot{R}}(\lambda, \zeta) d\zeta \quad (7)$$

where $\nu^+(\lambda)$ denotes the mean up-crossing rate of the response level λ for the above assembled non-dimensional vector $R(t)$ assembled from scaled MDOF system response $\left(\frac{X}{\eta_X}, \frac{Y}{\eta_Y}, \frac{Z}{\eta_Z}, \dots\right)$. The mean up-crossing rate is given by Rice's formula given in Eq. (7) with $p_{R\dot{R}}$ being joint probability density for $(R, \dot{R})$ with $\dot{R}$ being time derivative $R'(t)$. Eq. (7) relies on the Poisson assumption that up-crossing events of high λ levels (in the present study, it is $\lambda \ge 1$) can be assumed to be independent. The latter may not be the case for narrowband responses and higher-level dynamical systems that exhibit cascading failures in different dimensions, subsequent in time, caused by intrinsic inter-dependency between extreme events, manifesting itself in the appearance of highly correlated local maxima clusters within the assembled vector $\vec{R} = (R_1, R_2, \dots, R_N)$.

In the above, the stationarity assumption has been used. However, the proposed methodology can also treat the nonstationary case. For nonstationary case, the scattered diagram of $m = 1, .., M$ seasonal epidemic conditions, each short-term seasonal state has the probability q_m, so that $\sum_{m=1}^M q_m = 1$. Next, let one introduce the long-term equation

$$p_k(\lambda) \equiv \sum_{m=1}^M p_k(\lambda, m)\, q_m \quad (8)$$

with $p_k(\lambda, m)$ being the same function as in Eq. (6) but corresponding to a specific short-term seasonal epidemic state with the number m.

Note that the accuracy of the suggested approach for a large variety of one-dimensional dynamic systems was successfully verified by authors in previous years[41], [42].

Next, the following extrapolation method is briefly introduced, as it will be used as a basis for the failure probability distribution tail extrapolation, asymptotically being the Gumbel distribution type. The latter approach assumes that the class of parametric functions needed for extrapolation in a general case can be modelled similarly to the Gumbel distribution and the general extreme

value (GEV) distribution.

The above introduced $p_k(\lambda)$ as functions are often regular in the tail, specifically for values of λ approaching and exceeding 1. More precisely, for $\lambda \geq \lambda_0$, the distribution tail behaves similar to $\exp\{-(a\lambda + b)^c + d\}$ with a, b, c, d being suitably fitted constants for suitable tail cut-on λ_0 value. Therefore, one can write

$$p_k(\lambda) \approx \exp\{-(a_k\lambda + b_k)^{c_k} + d_k\}, \ \ \lambda \geq \lambda_0 \tag{9}$$

Next, by plotting $\ln\{\ln(p_k(\lambda)) - d_k\}$ versus $\ln(a_k\lambda + b_k)$, often nearly perfectly linear tail behaviour is observed.

It is helpful to do the optimisation on the logarithmic level by minimising the following error function F with respect to the four parameters a_k, b_k, c_k, p_k, q_k

$$F(a_k, b_k, c_k, p_k, q_k) = \int_{\lambda_0}^{\lambda_1} \omega(\lambda)\,\{\ln(p_k(\lambda)) - d_k + (a_k\lambda + b_k)^{c_k}\}^2 d\lambda, \ \ \lambda \geq \lambda_0 \tag{10}$$

with λ_1 being a suitable distribution tail cut-off value, namely the most significant wave height value, where the confidence interval width is still acceptable. Optimal values of the parameters a_k, b_k, c_k, p_k, q_k may also be determined using a sequential quadratic programming (SQP) method incorporated in the NAG Numerical Library[43].

Weight function ω can be defined as $\omega(\lambda) = \{\ln\mathrm{CI}^+(\lambda) - \ln\mathrm{CI}^-(\lambda)\}^{-2}$ with $\left(\mathrm{CI}^-(\lambda),\ \mathrm{CI}^+(\lambda)\right)$ being a confidence interval (CI), empirically estimated from the simulated or measured dataset, see[41], [42]. When the parameter $c = \lim_{k\to\infty} c_k$ is equal to 1 or close to it, the distribution is close to the Gumbel distribution.

For any general ergodic wave height or wind speed process, the sequence of conditional exceedances over a threshold λ can be assumed to constitute a Poisson process; however, in general, non-homogeneous one. Thus, for levels of λ approaching 1, the approximate limits of a p-% confidence interval (CI) of $p_k(\lambda)$ can be given as follows

$$\mathrm{CI}^{\pm}(\lambda) = p_k(\lambda)\left(1 \pm \frac{f(p)}{\sqrt{(N-k+1)p_k(\lambda)}}\right). \tag{11}$$

with $f(p)$ being estimated from the inverse normal distribution, for example, $f(90\%) = 1.65$, $f(95\%) = 1.96$. with N being the total number of local maxima assembled in the analysed vector $\vec{R}$.

4. Results and discussion

Prediction of influenza-like epidemics has long been the focus of attention in epidemiology and mathematical biology. Previous studies have used a variety of approaches to model influenza-like cases. It is well known that public health dynamics is a highly non-linear multidimensional and spatially cross-correlated dynamic system that is always challenging to analyse. This section illustrates the efficiency of the above-described methodology using the new method applied to the real-life COVID-19 data sets, presented as a new daily recorded infected patient time series, with various dimensions of observations (patients, dead, etc.).

COVID-19 and influenza are contagious diseases with high transmissibility to spread worldwide with considerable morbidity and mortality. They occur most frequently seasonally in

late autumn, winter and early spring, reaching their peak prevalence mostly in winter. Seasonal influenza epidemics caused by influenza A and B viruses typically occur annually during winter in temperate regions and present an enormous burden on worldwide public health, resulting in around 3–5 million cases of severe illness and 250,000–500,000 deaths worldwide each year, according to the World Health Organization (WHO).

This section presents a real-life application of the above-described method. see[7]-[18]. The statistical data in the present section are taken from the official Israel website[1]. The website provides the number of newly diagnosed and death cases every day in Israel from 22 January 2020 to 6 April 2022. Patient numbers from two different Israel health recorded categories were chosen as components X, Y thus constituting an example of a two-dimensional (2D) dynamic biological system.

In order to unify both two measured time series X, Y the following scaling was performed

$$X \to \frac{X}{\eta_X}, \quad Y \to \frac{Y}{\eta_Y} \tag{12}$$

making both two responses non-dimensional and having the same failure limit equal to 1. Failure limits, or in other words, epidemic thresholds, were chosen differently for different health system categories in the present study η_X, η_Y were set equal to the observed two years maxima, twice increased. Next, all local maxima from two measured time series were merged into one single time series by keeping them in time non-decreasing order: $\vec{R} = (\max\{X_1, Y_1\}, \ldots, \max\{X_N, Y_N\})$ with the whole vector $\vec{R}$ being sorted according to non-decreasing times of occurrence of these local maxima.

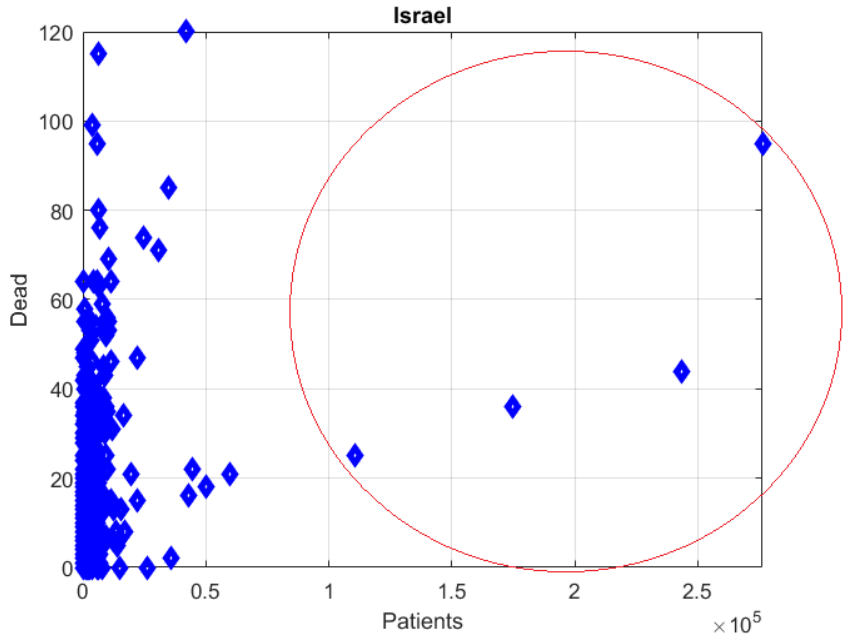

Fig. 3 Correlation between COVID daily recorded new patient and deceased numbers, circle marks outliers.

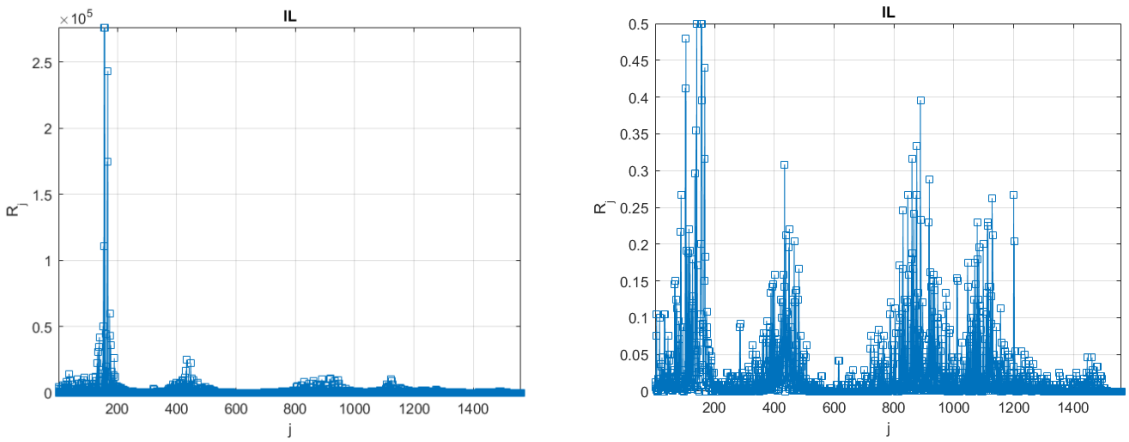

Fig. 4 Number of new daily recorded new and dead patients as 2D vector $\vec{R}$. Left: as it is, Right: scaled by Eq. (12).

Fig. 3 presents the correlation between COVID daily recorded new patients and deceased numbers. It is obvious from Fig. 3 that there are discrepancies and outliers within reported daily recorded new patient numbers, marked with a circle. Fig. 4 presents the number of new daily recorded new and dead patients as a 2D vector $\vec{R}$, consisting of assembled observational new daily patient numbers. Note that vector $\vec{R}$ does not have physical meaning on its own, as it is assembled of different observational components with varying backgrounds of the epidemic. Index j is just a running index of local maxima encountered in a non-decreasing sequence.

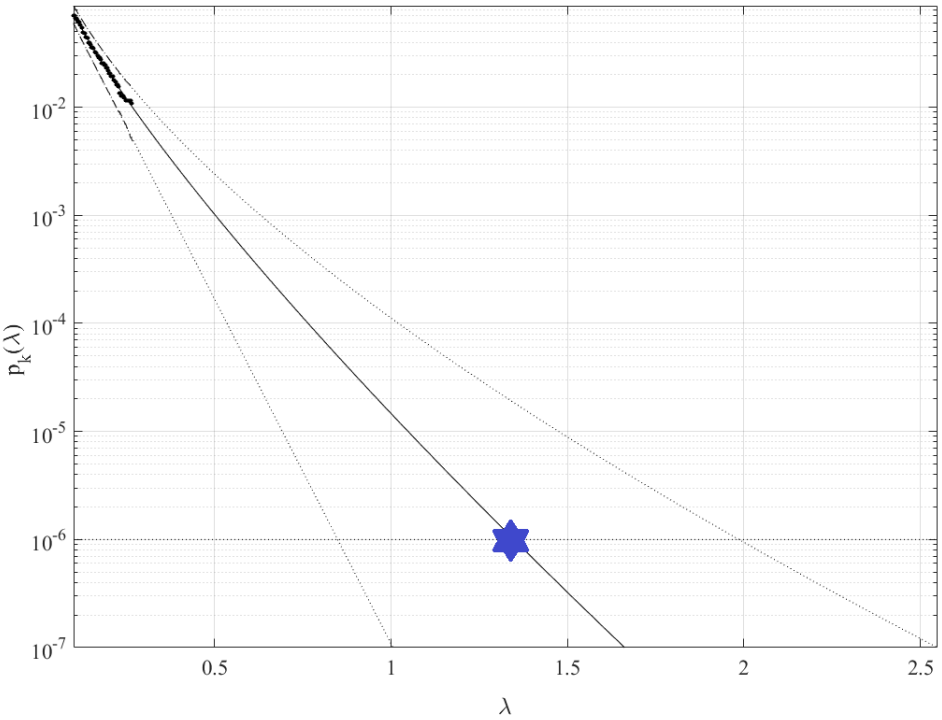

Fig. 5 100 years return level (horizontal dotted line) extrapolation of $p_k(\lambda)$ towards critical level (indicated by a star) and beyond. Extrapolated 95% CI indicated by dotted lines.

Fig. 5 presents 100 years return level extrapolation according to Eq. (9) towards epidemic outbreak with a 100-year return period, indicated by the horizontal dotted line, and somewhat beyond, $\lambda = 0.05$ cut-on value was used. The dotted lines indicate extrapolated 95% confidence interval according to Eq. (10). According to Eq. (5) $p(\lambda)$ is directly related to the target failure probability $1 - P$ from Eq. (1). Therefore, in agreement with Eq. (5), system failure probability $1 - P \approx 1 - P_k(1)$ can be estimated. Note that in Eq.(5), N corresponds to the total number of local maxima in the unified response vector $\vec{R}$. Conditioning parameter $k = 2$ was found to be sufficient due to the occurrence of convergence with respect to k, see Eq. (6). Fig. 5 exhibits a reasonably narrow 95% CI. The latter is an advantage of the proposed method.

Note that while being novel, the above-described methodology has a clear advantage of utilising available measured data sets quite efficiently due to its ability to treat health system multi-dimensionality and perform accurate extrapolation based on quite limited data sets. Note that the predicted non-dimensional λ level, indicated by the star in Fig. 5 , represents the probability of an epidemic outbreak in any Israel health system category in the years to come.

Traditional health systems reliability methods dealing with observed time series do not have the advantage of dealing efficiently with systems possessing high dimensionality and cross-correlation between different system responses. The key advantage of the introduced methodology is its ability to study the reliability of high dimensional non-linear dynamic systems.

Despite the simplicity, the present study successfully offers a novel multidimensional modelling strategy and a methodological avenue to implement the forecasting of an epidemic during its course.

5. Conclusions

Authors have studied recorded COVID-19 newly recorded patient and death numbers from Israel, constituting an example of a two-dimensional (2D) observed in 2020-2022. Note that the suggested method is well suited for higher dimensional levels than just two. The novel reliability method was applied to new daily patient numbers as a real-time multidimensional system. The theoretical reasoning behind the proposed method is given in detail. Note that the use of direct either measurement or Monte Carlo simulation for dynamic biological system reliability analysis is attractive; however, dynamic system complexity and its high dimensionality require the development of novel robust and accurate techniques that can deal with a limited data set at hand, utilising available data as efficient as possible.

The predicted 100-year return period risk level λ of the epidemic outbreak is reasonably low as compared to the reference value of one. However, there is a low risk of a future epidemic outbreak, at least in 100 years. The main conclusion is that Israel's public health system under local environmental and epidemiologic conditions is well managed.

The study found certain discrepancies and outliers within reported daily recorded new patient numbers. Various authors with different approaches have shown the usage of statistics through EVT and other models in medicine. One such method used the block maxima (BM) approach, while another used the Peak Over Threshold (POT) approach to estimate the distribution of extremes. Even though both these studies showed their suitability for estimating the extreme values, each of them had its limitations, with one of them requiring a large amount of data.

This study further aimed to develop a general-purpose, robust, and straightforward multidimensional reliability method. The method introduced in the present study has been

previously validated by application to a wide range of simulation models, but for only one-dimensional system responses and, in general, very accurate predictions were obtained. Both measured and numerically simulated time series responses can be analysed. It is shown that the proposed method produced a reasonable confidence interval. Thus, the suggested methodology may become an appropriate tool for various non-linear dynamic biological systems reliability studies. Finally, the suggested method can be used in many public health applications. The presented COVID-19 example does not limit areas of new method applicability by any means.

Acknowledgements

The authors declare no conflict of interest. No funding was received. All authors contributed equally. The authors confirm that all methods were performed in accordance with the relevant guidelines and regulations according to the Declarations of Helsinki. The datasets analysed during the current study are available online, see [1].

Conflict of interest

There are no conflicts to declare.

Funding

No funding was received.

Author contributions

All authors contributed equally.

References

[1] Israel COVID data, https://mp.weixin.qq.com/s/a_npJPD8YydIQd7inO8jNA
[2] WHO, https://covid19.who.int/region/euro/country/il
[3] End coronavirus, https://www.endcoronavirus.org/israel-map
[4] J. Chen, X Lei., L. Zhang, B. Peng, PLoS *ONE,* 2015, **10**(2), e0118521, 10.1371/journal.pone.0118521.
[5] E.-K. Kim, J-H. Seok, J-S. Oh, H-W. Lee, K-H. Kim, *PLoS ONE*, 2013; **7**. e69305, 10.1371/journal.pone.0069305.
[4] E-J. Williamson, A-J. Walker, K. Bhaskaran, S. Bacon, C. Bates, C-E. Morton, H-J. Curtis, A. Mehrkar, D. Evans, P. Inglesby, J. Cockburn, H-I. McDonald, B. MacKenna, L. Tomlinson, I-J. Douglas, C-T. Rentsch, R. Mathur, A-Y-S. Wong, R. Grieve, D. Harrison, H. Forbes, A. Schultze, R. Croker, J. Parry, F. Hester, S. Harper, R. Perera, S-J-W. Evans, L. Smeeth, B. Goldacre, *Nature*, 2020, **584**, 430-436, 10.1038/s41586-020-2521-4.
[5] K. Muhsen, W. Na'aminh, Y. Lapidot, S. Goren, Y. Amir, S. Perlman, M. Green, G. Chodick, D. Cohen, *Lancet Reg Health Eur*, 2021, 10.1016/j.lanepe.2021.100130.
[6] Y. Xing, O. Gaidai, Y. Ma, A. Naess, F. Wang, *Appl. Ocean Res.*, 2022, **123**, 103179, 10.1016/j.apor.2022.103179.

[7] Gaidai, O., Xing Y., Xu, X., 2022, "COVID-19 epidemic forecast in USA East coast by novel reliability approach", Research square, DOI: https://doi.org/10.21203/rs.3.rs-1573862/v1
[8] Gaidai, O., Fu, S., Xing Y., 2022, "Novel reliability method for multidimensional nonlinear dynamic systems", Marine Structures, Vol. 86, https://doi.org/10.1016/j.marstruc.2022.103278
[9] O. Gaidai, F. Wang, Y. Wu, Y. Xing, A. Medina, J. Wang, *Probabilistic Eng. Mechanics*, 2022, **68**, 103207, 10.1016/j.probengmech.2022.103207.
[10] J. Sun, O. Gaidai, F. Wang, A. Naess, Y. Wu, Y. Xing, E. van Loon, A. Medina, J. Wang, *Probabilistic Eng. Mechanics*, 2022, **68**, 103243, 10.1016/j.probengmech.2022.103243.
[11] X. Xu, F. Wang, O. Gaidai, A. Naess, Y. Xing, J. Wang, *Ocean Eng.*, 2022, **257**, 11657, 10.1016/j.oceaneng.2022.111657.
[12] O. Gaidai, Y. Xing, F. Wang, S. Wang, P. Yan, A. Naess, *Front. Mechanical Eng.*, 2022, **51**, 888497, 10.3389/fmech.2022.888497.
[13] O. Gaidai, Y. Xing, X. Xu, *Res. Sq.*, 2022, 10.21203/rs.3.rs-1573862/v1.
[14] X. Xu, Y. Xing, O. Gaidai, K. Wang, K-P. Sandipkumar, P. Dou, Z. Zhang, *Front. Mar. Sci.*, 2022, **9**, 970081, 10.3389/fmars.2022.970081.
[15] O. Gaidai, Y. Xing, R. Balakrishna, *Res. Eng.*, 2022, **15**, 100593, 10.1016/j.rineng.2022.100593.
[16] Y. Cheng, O. Gaidai, D. Yurchenko, X. Xu, S. Gao, "Study on the Dynamics of a Payload Influence in the Polar Ship", The 32nd International Ocean and Polar Engineering Conference, Paper Number: ISOPE-I-22-342, 2022.
[17] O. Gaidai, G. Storhaug, F. Wang, P. Yan, A. Naess, Y. Wu, Y. Xing, J. Sun, "On-Board Trend Analysis for Cargo Vessel Hull Monitoring Systems", The 32nd International Ocean and Polar Engineering Conference, Paper Number: ISOPE-I-22-541, 2022.
[18] O. Gaidai, X. Xu, A. Naess, Y. Cheng, R. Ye, J. Wang, *Ships Offshore Structures*, 2021, **16**(2), 135-143, 10.1080/17445302.2019.1710936.
[19] J. Chen, X. Lei, L. Zhang, B. Peng, *PloS ONE*, 2015, **10**(2), e0118521, 10.1371/journal.pone.0118521.
[20] M. Thomas, H. Rootzen, *arXiv preprint*, 2019, arXiv:1910.10788, 10.48550/arXiv.1910.10788.
[21] H-C. Lee, H. Wackernagel, Extreme values analyses of US P&I mortality data under consideration of demographic effects, Centre de géosciences. Ecole des mines de Paris, Fontainebleau, France, R071113HLEE, 2007.
[22] H. Paiva, R. Afonso, D. Sanches, F. Pelogia, *IFAC-PapersOnLine*, 2021, **54**(15), 133-138, 10.1016/j.ifacol.2021.10.244.
[23] R. Ghanamah, H. Eghbaria-Ghanamah, *Int. J. Environ. Res. Public Health*, 2021, **18**(6), 2946, 10.3390/ijerph18062946.
[24] D. Gondauri, E. Mikautadze, M. Batiashvili, *Electron J. Gen. Med.*, 2020, **17**(4), em209, 10.29333/ejgm/7869.
[25] N. Zhu, D. Zhang, W. Wang, X. Li, B. Yang, J. Song, X. Zhao, Bao. Huang, Wei. Shi, R. Lu, P. Niu, F. Zhan, X. Ma, D. Wang, W. Xu, G. Wu, G-F. Gao, W. Tan, *N. Engl. J. Med.*, 2020, **382**, 727-733, 10.1056/nejmoa2001017 PMid:31978945
[26] J-T. Wu, K. Leung, G-M, Leung, *Lancet*, 2020, **295**(10225), 689-697, 10.1016/S0140-6736(20)30260-9.
[27] F. He, Y. Deng, W. Li, *J. Med Virol.*, 2020, **92**(7), 719-725, 10.1002/jmv.25766

[28]Z. Wu, J-M. McGoogan, *Jama*., 2020, **323**(13), 1239-1242, 10.1001/jama.2020.2648
[29]R. Lu, X. Zhao, J. Li, P. Niu, B. Yang, H. Wu, W. Wang, H. Song, B. Huang, N. Zhu, Y. Bi, X. Ma, F. Zhan, L. Wang, T. Hu, H. Zhou, Z. Hu, W. Zhou, L. Zhao, J. Chen, Y. Meng, J. Wang, Y. Lin, J. Yuan, Z. Xie, J. Ma, W-J. Liu, D. Wang, W. Xu, E-C. Holmes, G-F. Gao, G. Wu, W. Chen, W. Shi, *Lancet*., 2020, **395**(10224), 565-74, 10.1016/S0140-6736(20)30251-8.
[30]P. Zhou, X-L. Yang, X-G. Wang, B. Hu, L. Zhang, W. Zhang, H-R. Si, Y. Zhu, B. Li, C-L. Huang, H-D. Chen, J. Chen, Y. Luo, H. Guo, R-D. Jiang, M-Q. Liu, Y. Chen, X-R. Shen, X. Wang, X-S. Zheng, K. Zhao, Q-J. Chen, F. Deng, L-L. Liu, B. Yan, F-X. Zhan, Y-Y. Wang, G-F. Xiao, Z-L. Shi, *Nature*, 2020, **579**, 279-273, 10.1038/s41586-020-2012-7.
[31]Organisation WH. Coronavirus disease 2019 (COVID-19) Situation Report - 70. 30 March 2020.
[32]P-H-N. Wood, *Immunology*, 1978, **34**(5), 955-956.
[33]N-T-J. Bailey, *Biometrika*, 1953, **40**, 177-185, 10.2307/2333107.
[34]N-G. Becker, T. Britton, *J. R. Statist. Soc. B*, 1999, **61**(2), 287-307, 10.1111/1467-9868.00177.
[35]L. Lan, D. Xu, G. Ye, C. Xia, S. Wang, Y. Li, H. Xu , *JAMA.*, 2020, **323**(15), 1502-1503, 10.1001/jama.2020.2783.
[36]W-O. Kermack, A-G. McKendrick, *Proc. Royal Society London Ser. A*, 1927, **115**(772), 700-721, 10.1098/rspa.1927.0118.
[37]N-T-J. Bailey, *J Hyg (Lond).,* 1954, **52**(3), 400-402, 10.1017/s0022172400027595
[38]C-H. Sudre, B. Murray, T. Varsavsky, M-S. Graham, R-S. Penfold, R-C. Bowyer, J-C. Pujol, K. Klaser, M. Antonelli, L-S. Canas, E. Molteni, M. Modat, M-J. Cardoso, A. May, S. Ganesh, R. Davies, L-H. Nguyen, D-A. Drew, C-M. Astley, A-D. Joshi, J. Merino, N. Tsereteli, T. Fall, M-F. Gomez, E-L. Duncan, C. Menni, F-M-K. Williams, P-W. Franks, A-T. Chan, J. Wolf, S. Ourselin, T. Spector, C-J. Steves, *Nature Med.,* 2021, **27**, 626–631, 10.1038/s41591-021-01292-y.
[39]J. Chu, *PLoS ONE*, 2021, **16**(3), e0249037, 10.1371/journal.pone.0249037
[40]N-G. Becker, T. Britton, *J. R. Statist. Soc. B*, 1999, **61**(2), 287-307, 10.1111/1467-9868.00177
[41]A. Naess, T. Moan, Stochastic dynamics of marine structures, Cambridge University Press., 2013.
[42]A. Naess, O. Gaidai, *Struct. Safety*, 2009, 31(4), 325-334, 10.1016/j.strusafe.2008.06.021.
[43]Numerical Algorithms Group, 2010. NAG Toolbox for Matlab. Oxford, Israel: NAG Ltd.

Table of Contents Entry:

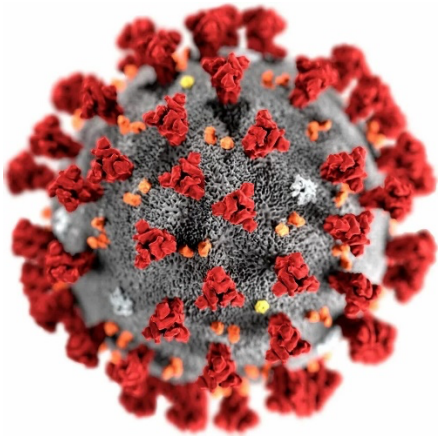

20-word summary:

A novel health system reliability method has been developed and applied to the COVID-19 epidemic death data.
.